Parasite strain coexistence in a heterogeneous host population

Darren M. Green, Istvan Z. Kiss and Rowland R. Kao

Heterogeneity in host susceptibility and transmissibility to parasite attack allows a lower transmission rate to sustain an epidemic than is required in homogeneous host populations. However, this heterogeneity can leave some hosts with little susceptibility to disease, and at high transmission rates, epidemic size can be smaller than for diseases where the host population is homogeneous. In a heterogeneous host population, we model natural selection in a parasite population where host heterogeneity is exploited by different strains to varying degrees. This partitioning of the host population allows coexistence of competing parasite strains, with the heterogeneity-exploiting strains infecting the more susceptible hosts, in the absence of physiological tradeoffs and spatial heterogeneity, and even for markedly different transmission rates. In our model, intermediate-strategy parasites were selected against: should coexistence occur, an equilibrium is reached where strains occupied only the extreme ends of trait space, under appropriate conditions selecting for lower R_0.

D. M. Green (darren.green@zoo.ox.ac.uk), I. Z. Kiss and R. R. Kao, Dept of Zoology, Univ. of Oxford, South Parks Road, Oxford, UK, OX1 3PS.

The ecology and evolution of parasites has important consequences for wildlife diseases, for diseases of domesticated animals and crops, and for human health (Schrag and Wiener 1995). Epidemiological theory suggests that parasites will evolve to maximise their basic reproduction number R_0 (Anderson and May 1982). In a homogeneously mixed population, this is defined as "the average number of secondary infections produced when one infected individual is introduced into a wholly susceptible host population at equilibrium" (Anderson and May 1991). The assumption of homogeneous mixing is an important one, which impacts not only on R_0, but also upon final epidemic size or equilibrium prevalence (Kiss et al. 2006a). Variation in host susceptibility and transmissibility constitutes a departure from this paradigm. Such heterogeneity can result from physiological differences such as variation in strength of immune response, or from behavioural differences producing variation in contact rates amongst individuals as is typically found in the contact networks of sexually transmitted infections (STIs; Lloyd-Smith et al. 2005).

Heterogeneity in susceptibility is frequently encountered in contact-network models of disease spread (Yorke et al. 1978, Newman 2002). Populations with higher heterogeneity in host-host contact rate, provided there is a positive correlation between susceptibility and infectiousness, have a lower threshold in the transmission rate for which an epidemic can occur (May and Lloyd 2001). Without a correlation between susceptibility and infectiousness, heterogeneity has no effect on the threshold. However, high heterogeneity implies that some individuals may be poorly connected and less easily infected. For high transmission rates, final epidemic size found on heterogeneous networks is lower than that found on homogeneous networks (Kiss et al. 2006a), as is the prevalence for models of endemic diseases.

Diseases with different transmission strategies will perceive different patterns of host contact. For example,

an STI will often perceive a more heterogeneous contact structure than an aerosol-borne disease (Liljeros et al. 2003). Likewise, it has been suggested that endemic diseases tend towards lower infectiousness over longer infectious periods as compared with epidemic diseases (Frank 1996), thus experiencing a more homogeneous host environment favouring higher prevalence at the expense of a higher initial rate of spread. Such a shift to lower viral replicative fitness may be occurring currently in HIV-1 (Arien et al. 2005), which, should this be combined with a longer infectious period, would imply a relatively increased risk to those in long-term sexual partnerships (Kao 2006). Similarly, recent changes in the frequencies of different strains of hepatitis C have been associated with increased intravenous drug use and decreased transmission via blood transfusions (Bourlière et al. 2002, Schröter et al. 2002), demonstrating a response by the pathogen to changing behavioural patterns in the host.

The same principles apply for spread of disease between populations in a metapopulation context. Foot-and-mouth disease (FMD) is transmitted between individual farms through varied routes for transmission, including movement of infected animals, fomites (objects that can harbour an infectious agent), and long-distance aerosol spread. Its transmission is highly variable and different livestock species are differentially susceptible to different FMD strains (Haydon et al. 2004). Transmission via aerosol-borne virus, as was important in the 1967 UK epidemic, is unlikely to show high levels of heterogeneity in the contact structure (Haydon et al. 2004). Infection in the UK in 2001 spread initially through the highly connected and heterogenous network of sheep trading movements (Gibbens et al. 2001).

The host population therefore represents, to competing parasites, a complex structured resource where individuals are differentially susceptible to different parasites types or species. Such resource partitioning has also been shown to promote species coexistence (Wilson et al. 1999, Bonsall et al. 2002), and host heterogeneity allows parasite coexistence by providing 'refuges' that favour different parasite strains (Li et al. 2003). Thrall and Antonovics (1997) found that pathogens with different patterns of host contact can coexist without spatial or host heterogeneity.

With heritable genetic variation in transmission strategy, parasites might evolve to maximise their evolutionary success. Kao (2006) considered the exploitation of heterogeneity as a heritable trait, and showed that, in a deterministic setting, selection on the parasite population can result in the parasite evolving away from exploitation of host heterogeneity, even where this involves a reduction in R_0. He showed also that a single competing strain that exploits heterogeneity and thus has higher R_0 is able to invade, but may itself evolve towards lower R_0.

Here, we consider further the evolution of transmission strategies through different host contact structures, with a strain-based model of host-parasite interactions that allows competition between, and coexistence of competing multiple strains with different transmission rates and strategies. This is modelled stochastically using individual-based simulation and deterministically through an equivalent set of differential equations. We consider a heterogeneous host population, subject to infection by 'specialist' parasites that exploit the heterogeneity, and 'generalist' parasites that do not. We show that coexistence of parasite strains with different strategies is possible with neither explicit tradeoffs, nor local spatial structure, but that intermediate-strategy parasites never persist.

Model

The mean-field model

The model is derived from the well known SIS host-pathogen model, (discussed by Anderson and May 1991) where individuals are either susceptible or infected, and once recovered are immediately susceptible again. Alternatively, recovery may represent death of infected individuals matched by a birth rate sufficient to keep the population size constant. We assume complete cross-immunity between parasite types throughout.

$$\frac{dI}{dt} = \beta SI - \gamma I \qquad (1)$$

Here, S and I are the proportions of susceptible and infected hosts respectively, such that $S+I=1$, and γ and β are the rates of recovery and infectious contact per infected individual. The mean infectious period length is γ^{-1}.

In the ecological literature, R_0 pertains to the reproduction number at any equilibrium (Mylius and Diekmann 1995); however in the epidemiological literature, it specifically represents the reproduction number in an entirely susceptible population (Anderson and May 1991). Below, we qualify R_0 by specifying the population concerned: $R_0(x,s)$ represents the reproduction number of a parasite x at an equilibrium with s susceptible individuals available for infection. As a shorthand, we denote R_0 in an entirely susceptible population simply by $R_0(x)$. For the mean field model, it can easily be shown that in an entirely susceptible population, $R_0(MF) = \beta/\gamma$, and that at equilibrium,

$$S^* = \frac{\gamma}{\beta} \qquad (2)$$

Heterogeneity in host susceptibility

We now consider a heterogeneous host population where individuals possess an 'h-state variable' ξ (Diekmann et al. 1990). In the context of an STI, this could represent the number of sexual contacts an individual has; for a metapopulation (farm-based) model of FMD, the number of trading movements made. More generally, ξ represents at once the relative infectivity and susceptibility of hosts, assumed completely correlated with proportionate mixing. The situation where infectivity and susceptibility are less strongly correlated is considered in Appendix 1. Under proportionate mixing, contacts between pairs of individuals are randomly allocated proportionately to the product of their values of ξ. We denote the number distributions of the total population, susceptible population, and infected population as n, s, and i respectively, and the density of the total population in class a ($a \in \{s,i,n\}$) with infectivity ξ as a_ξ, where $\xi \in \Omega$ and $\Omega = [0, \infty]$. Thus $i_\xi + s_\xi = n_\xi$; and $\int_\Omega s_\xi d\xi = S$, $\int_\Omega i_\xi d\xi = I$ and $\int_\Omega n_\xi d\xi = 1$. (Therefore, though we describe s and i as 'distributions', they do not generally sum to one.)

To allow a controlled comparison between models below, we normalise ξ such that its expectation is unity:

$$\int_\Omega \xi n_\xi d\xi = 1$$

The differential equation model for the SIS model with heterogeneous transmission is therefore given by the set of differential equations

$$\frac{di_\xi}{dt} = \beta \xi s_\xi \int_\Omega x i_x dx - \gamma i_\xi, \quad \xi \in \Omega \quad (3)$$

The population is at equilibrium when for all ξ, $\frac{di_\xi}{dt} = 0$.

Such distributed-parameter SIS models have no general analytical solution, though they do exist for specific cases such as the mean-field model (Eq. 1). However, for a specified distribution n, the unique equilibrium in the presence of disease can be found through numerical approximation of this infinite set of equations. The equilibrium distributions of infected and susceptible hosts are denoted below by i* and s*, with totals I* and S*.

Heterogeneity in parasite attack

The models presented above (Eq. 1 and 3) are special cases of the following more general model. Following Kiss et al. (2006a), we consider the parasite population to possess a parameter λ that determines the degree to which it exploits host heterogeneity ($\lambda \in [0,1]$). This parameter represents the transmission strategy which a particular parasite strain adopts. In the context of FMD, λ could represent a sliding scale of strain types, between strains where aerosol spread is important,

through to strains where pigs are less affected and aerosol spread lower, but with increased susceptibility in sheep. Where $\lambda = 0$, the model is equivalent to Eq. 3 above, with the parasite able to exploit the full range of host heterogeneity. For $\lambda = 1$, parasite transmission is an entirely homogeneous process independent of the host heterogeneity ξ, and the model is an equivalent of the mean-field model Eq. 1. Therefore,

$$\frac{di_\xi}{dt} = \lambda \beta^1 s_\xi \int_\Omega i_x dx + (1-\lambda)\beta^0 \xi s_\xi \int_\Omega x i_x dx - \gamma i_\xi \quad \xi \in \Omega \quad (4)$$

where β^0 and β^1 denote the transmission rate for the fully heterogeneous ($\lambda = 0$) and homogeneous ($\lambda = 1$) transmission mechanisms respectively, assuming a linear relationship between λ and β for intermediate λ:

$$\beta^\lambda = \lambda \beta^1 + (1-\lambda)\beta^0 \quad (5)$$

The equilibrium state for a single strain λ, $i*(\lambda)$ can again be found by numerical solution of this set of equations. Appendix 1 shows the derivation of R_0 for this general model, the form of which is shown below, where $\langle a^n \rangle = \int_\Omega \xi^n a_\xi d\xi$.

$$R_0(\lambda, s) = \left(\lambda \beta^1 S + (1-\lambda)\beta^0 \langle s^2 \rangle \right.$$

$$\left. + \sqrt{[\lambda \beta^1 S - (1-\lambda)\beta^0 \langle s^2 \rangle]^2 + 4\lambda(1-\lambda)\beta^1 \beta^0 \langle s^1 \rangle^2} \right) \Big/ 2\gamma$$

$$(6)$$

We denote R_0 for a particular parasite strain λ with a given distribution of available susceptibles s as $R_0(\lambda,s)$, with shorthand $R_0(\lambda)$ for an entirely susceptible population (s = n). For $\lambda = 1$ and $\lambda = 0$, Eq. 6 simplifies as expected: $R_0(1) = \frac{\beta^1}{\gamma}$ and $R_0(0) = \frac{\beta^0}{\gamma} \langle n^2 \rangle$.

Simulation and equilibria

Introducing a parasite strain λ into a population maintaining an epidemic of a resident parasite strain $\hat{\lambda}$ (at equilibrium) is analogous to that of introducing parasite λ into the disease-free state. However, though for the disease-free state the available population of susceptibles in which λ can invade was n, it is now that of the equilibrium $s*(\hat{\lambda})$. In general, the equilibrium population of $\hat{\lambda}$ can be invaded by λ if and only if $R_0(\lambda, s*(\hat{\lambda})) > 1$, and strain $\hat{\lambda}$ is an evolutionary stable strategy (ESS) if no other strain λ can invade it (Maynard Smith and Price 1973). However, certain properties such as positive density dependence (Allee 1931), not included in this model, would invalidate the assumption that $R_0 = 1$ is the global threshold. As a condition of the equilibrium, $R_0(\hat{\lambda}, s*(\hat{\lambda})) = 1$ (Mylius and Diekmann 1995). If a strain can invade a resident strain, coexistence may be possible, but where $R_0(\lambda, s*(\hat{\lambda}))$ for an invading strain is above, but close

to unity, the invading strain λ may reach a small population size only.

Below, we consider two distributions of hosts n shown in Table 1. Both distributions have equal $\langle n^1 \rangle = 1$ and equal $\langle n^2 \rangle$. The range of ξ was made finite with a possible range $\Omega = (0,10)$ and divided into 1000 bins to allow numerical solution of the equations.

The numerical solutions of the Eq. 4 and 6 were complemented by individual-based simulation allowing for natural selection of competing parasite strains, using one of the host population structures from Table 1. A population size of N = 2000 was used, with γ = 1.0. Each individual was assigned a value of ξ chosen from the exponential distribution with mean 1.0 according to $\xi_j = -\ln(\varepsilon_j)$ where ε represents numbers chosen from a uniform distribution in the range (0,1). Simulation was by synchronous updating with a step size of 0.01. Two parasite population structures are considered: in the multiple-strain model, parasites of all values of λ may exist across the full range of [0,1], as might be the case where λ is a quantitative trait; in the two-strain model, only parasites at the two extremes, λ = 0 and λ = 1 were allowed, simulating two distinct strains or a one-locus, two-allele system.

Epidemics were seeded with 100 randomly selected index cases, each with a value of λ to denote the parasite type infecting them. For the two-strain simulation, half had λ = 0 and half λ = 1. Daughter infections inherited λ from their parent infection, with a probability m of mutation to the other strain each infection event. A multiple-strain simulation was initialised with each seed's value of λ chosen randomly from the uniform distribution over the range [0,1], giving an initial population containing individuals from a range of strains. Here, for a daughter case ν infected by a case u, $\lambda_\nu = \lambda_u + \sigma_\lambda \varepsilon$ where σ_λ scales the mutation rate and ε is chosen from the standard normal distribution, subject to the constraint $0 \le \lambda_j \le 1$.

For the individual-based model, transmission between each possible pair of infected (u) and suspectible (v) individuals is considered at each time-step, and infection across each pair occurs at a rate τ:

$$\tau_{uv} = \lambda_u \frac{\beta^1}{N} + (1 - \lambda_u) \frac{\beta^0 \xi_u \xi_v}{N} \qquad (7)$$

Table 1. Distributions of ξ.

Distribution	n_ξ		$\langle n^2 \rangle$
Homogeneous model (i.e. λ = 1)	1	ξ = 1	1
	0	ξ ≠ 1	
Exponential	$\exp(-\xi)$		2
Bimodal	$\frac{1}{2}$	|ξ − 1| = 1	2
	0	|ξ − 1| ≠ 1	

Results

Equilibria

Numerical solutions for the equilibrium prevalence for purely heterogeneous (λ = 0), purely homogeneous (λ = 1), and intermediate types of contact are shown in Fig. 1 for the exponential distribution of ξ, matching the result of Kiss et al. (2006a). At β/γ ≈ 1.75, equilibrium prevalence is equal for all the models. Unlike R_0, equilibrium prevalence cannot be determined from the first and second moments $\langle n^1 \rangle$ and $\langle n^2 \rangle$: the bimodal distribution of ξ suffers smaller epidemics at equilibrium than the exponential distribution of ξ, despite having both the same transmission rate β and the same $R_0(\lambda)$.

Equilibrium behaviour is shown in Fig. 2 for different values of β and both distributions of ξ (Table 1, Eq 6). Numerical solutions of Eq. 4 for the two-strain model (Fig. 2a) are shown alongside simulation results for the two-strain (Fig. 2b) and multiple-strain (Fig. 2c) models (Eq. 7). In Fig. 2a, regions A and B indicate where only one strain can cause an epidemic in a completely susceptible population ($R_0(\lambda) > 1$). However, for markedly different β values, one strain cannot invade the other when the other is already at equilibrium and coexistence is not expected: (Regions A [B] and B [A]: $R_0(\lambda, s^*(1-\lambda)) < 1$). Between these regions, both strains can invade each other when the other strain is at equilibrium, and thus coexistence is expected (Region A B). From Eq. 2 and 6, the upper boundary of this region is $\beta^0 \langle n^2 \rangle = \beta^1$. The lower boundary differs between distributions of ξ and requires numerical solution. For the bimodal distribution, equilibrium prevalence by the heterogeneous-transmission strain at higher transmission rates is lower than that for the exponential distribution. Thus, this equilibrium can be more readily invaded by the homogeneous-transmission strain, and the region of coexistence is larger.

Figure 2b and 2c show individual-based simulation results. Coexistence of multiple strains occurs where
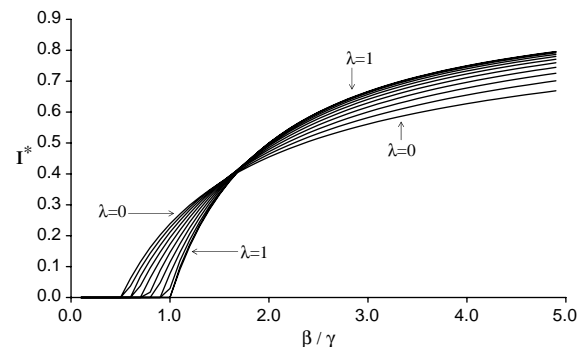
Fig. 1. Plot of I* versus β/γ for $\beta^0 = \beta^1 = \beta$ and an exponential distribution of ξ showing the solutions for different λ.
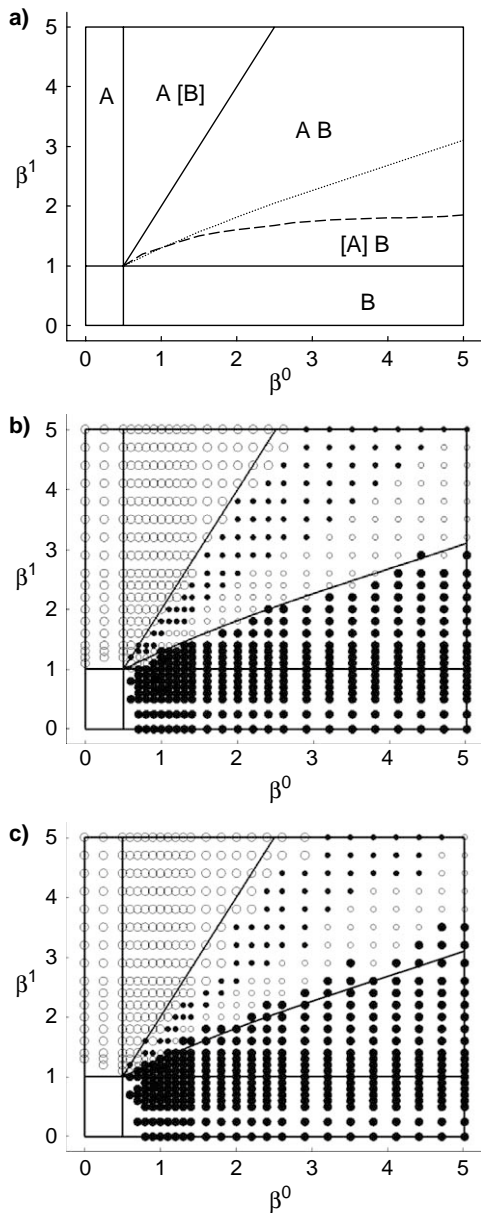
Fig. 2. Contour plot showing regions of persistence and coexistence of purely specialist ($\lambda = 0$) and purely generalist ($\lambda = 1$) types. x-axis: β^0; y-axis: β^1. $\gamma = 1$. (a) In regions marked A and B, the generalist and specialist types can spread in the susceptible population (A: $R_0(1) > 1$; B: $R_0(0) > 1$). Where a type is indicated in brackets, it cannot spread in a population where the other type is at equilibrium ($R_0(\lambda, s^*(1-\lambda)) < 1$) and thus no coexistence is possible. Dotted line: lower bound of coexistence region for exponential distribution of ξ; dashed line: lower bound for bimodal distribution. (b) As in (a), with overlaid individual-based simulation results for two-strain model with $m = 0.01$ and exponential distribution of ξ. Points indicate mean population λ at equilibrium, $\bar{\lambda}$. Large white symbols: $\bar{\lambda} > 0.9$; small black symbols: $0.5 < \bar{\lambda} < 0.9$; small white symbols: $0.1 < \bar{\lambda} < 0.5$; large black symbols: $\bar{\lambda} < 0.1$. (c) Overlaid individual-based simulation results for multiple-strain model with $\sigma_\lambda = 0.01$. Symbols as in (b).

mean λ at equilibrium, $\bar{\lambda}$, lies between zero and one. The region where coexistence was found closely matches that predicted by Eq. 6. No sharp switching in model behaviour was seen: $\bar{\lambda}$ varies smoothly between the upper and lower boundaries of this region, though the region itself is smaller for smaller β values.

Results for the multiple-strain simulation (Fig. 2c) closely resemble those for the two-strain case (Fig. 2b). This is as a result of the evolution of the strain structure through time: as the population approaches its equilibrium configuration, it consists mainly of individuals with the extreme values of λ (zero and one), with a few intermediate forms produced by random drift inwards from the extremes. An example of such a time-course for a simulation is shown in Fig. 3. Intermediate values of λ are never stable strategies, as explained below. The heterogeneous transmission parasites tended to infect hosts with higher values of λ, similar to the 'hierarchical spread' of disease through well-connected nodes in a network-based SIR model (Barthélemy et al. 2004, Kiss et al. 2006b).

Stability

Figure 4 demonstrates that strains with intermediate values of λ will always be invaded by strains with extreme values of $\lambda = 0$ and $\lambda = 1$. This contour plot shows the values of R_0 for each possible strain λ when introduced into a population of hosts at equilibrium infected by parasites of a second strain $\hat{\lambda}$, i.e. $R_0(\lambda, s^*(\hat{\lambda}))$. Here, we consider $\beta^0/\gamma = \beta^1/\gamma = 3$, representing a single point on Fig. 1 and 2 within the A B region of coexistence. By definition, on the diagonal, $R_0(\hat{\lambda}, s^*(\hat{\lambda})) = 1$. In the case of the two-strain simulation, only the four corners of the contour plot are relevant: Both $R_0(0, s^*(1))$ and $R_0(1, s^*(0))$ exceed 1, confirming that the two strains may coexist.

For the multiple-strain simulation, the daughter cases of an individual with strategy $\hat{\lambda}$ can have a different strategy λ, but the difference $|\lambda - \hat{\lambda}|$ is small and dependent upon the mutation rate σ_λ and its distribution. Thus, the behaviour of $R_0(\lambda, s^*(\hat{\lambda}))$ where $\lambda \approx \hat{\lambda}$ on Fig. 4 is of interest. The upper boundary of Fig. 4 represents the fitness (R_0) of parasites introduced into a population at equilibrium where all parasites transmit by the homogeneous route. For all other strains along this line, $R_0 > 1$, and so invasion by strains with lower λ can occur. In individual-based simulations, invasion of $\lambda = 1$ by $\lambda < 1$ was seen when seeding was entirely at $\lambda = 1$, evolving towards $\lambda = 0$, unless the mutation rate was sufficiently low as to prevent selection.

The lower boundary of the contour plot represents the fitness of parasites introduced into a population at equilibrium where all parasites transmit by the
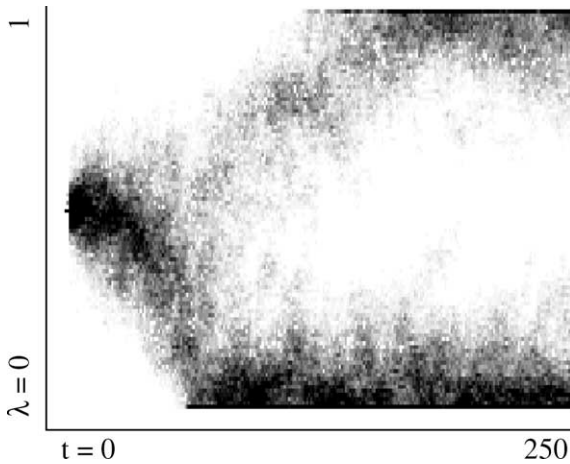
Fig. 3. Results for a single individual-based model simulation. Cross section of the distribution of λ through time (dark shading indicated more common strains) for one multiple-strain simulation starting with $\lambda = 0.5$ for all infectious individuals. $\beta^1/\gamma = \beta^0/\gamma = 4$, $\sigma_\lambda = 0.02$.

heterogeneous route. Here, for high λ, $R_0(\lambda, s^*(\hat{\lambda})) > 1$, though this R_0 is lower than that encountered at the opposite corner of the plot. However, a wide fitness minimum exists for intermediate values of λ (dotted line on Fig. 4) and $\lambda = 0$ is a local maximum for R_0. This minimum prevents invasion of the heterogeneous strategy parasites by other strategies except where the mutation rate is sufficiently high as to allow jumps over this minimum. In the individual-based simulations, $\lambda = 1$ individuals were never seen to emerge when seeding was entirely at $\lambda = 0$. When seeding was at random across all λ, in most cases the eventual outcome was coexistence at $\lambda = 0$ and $\lambda = 1$.
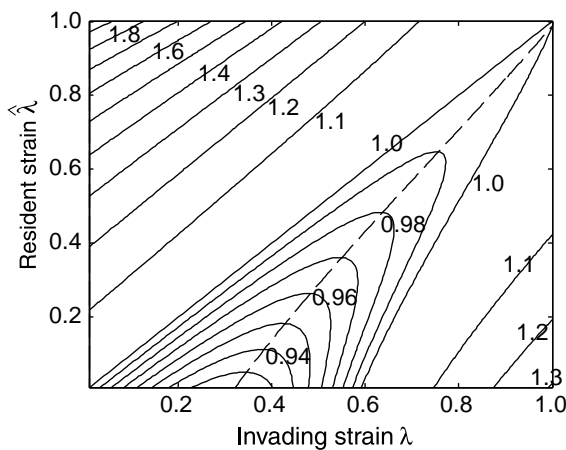
Fig. 4. Contour plot showing $R_0(\lambda, s^*(\hat{\lambda}))$ as a function of λ (x-axis) and $\hat{\lambda}$ (y-axis) for the exponentially distributed population. A dotted line indicates where the derivative $\frac{d}{d\lambda}R_0(\lambda, s^*(\hat{\lambda})) = 0$, representing $\min_\lambda R_0(\lambda, s^*(\hat{\lambda}))$.

Monomorphic approximation

Monomorphic approximations of the dynamics of complex evolutionary systems are commonly postulated (Dieckmann and Law 1996). Assuming divergent time-scales of evolutionary and population dynamics, a monomorphic approximation of the evolutionary dynamics of the model presented above (Eq. 4 and 6) was made, applying the canonical equation of adaptive dynamics (Dieckmann and Law 1996):

$$\frac{d\lambda}{dt} = \mu_\lambda \cdot \frac{\partial}{\partial \lambda'} R_0(\lambda', s^*(\lambda))\Big|_{\lambda' = \lambda}$$

where μ_λ scales the effects of the variability and heritability of the λ trait. An equilibrium exists where $\frac{\partial R_0}{\partial \lambda} = 0$ however, it is only stable for a negative second derivative: $\frac{\partial^2 R_0}{\partial \lambda^2}$. Values for $\frac{\partial R_0}{\partial \lambda}$ are shown in Fig. 5 for different values of β. For $\beta^1 = \beta^0$, an unstable equilibrium at $\lambda = 1$ is seen. A stable equilibrium here is not expected: in the individual-based model, the homogeneous strain was always seen to be invaded by heterogeneous strains. For lower β^0, equilibria do exist for intermediate λ, but these are always unstable. Though the boundaries $\lambda = 0$ and $\lambda = 1$ are fixed points in the monomorphic approximation, they are not ESSs in the individual-based model.

Discussion

Our results show that for a broad range of transmission rates, parasites that infect hosts through routes with and without heterogeneity can coexist in the absence of either life-history tradeoffs as they are usually implied, or local spatial structure. A form of tradeoff does exist in that individual transmission rates through the heterogeneous and homogeneous routes are correlated and depend upon λ. Local spatial structure can affect transmission rate (Rand et al. 1995, Read and Keeling 2003, van
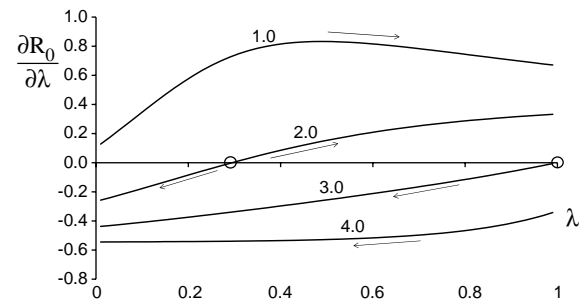
Fig. 5. Monomorphic approximations. Plot $\frac{\partial}{\partial \lambda} R_0(\lambda, s^*(\hat{\lambda}))$ versus λ for $\beta^1/\gamma = 3$ throughout at four different values of β^0/γ. Arrows indicate the trajectory of $\frac{d\lambda}{dt}$ for the monomorphic approximation. Unstable equilibria exist for $\frac{\partial R_0}{\partial \lambda} = 0$ (circled).

Ballegooijen and Boerlijst 2004) and may promote diversity in competing parasites (Buckee et al. 2004). In its absence, tradeoffs between transmissibility and other life-history traits similarly limit the evolution of high transmissibility (Messenger et al. 1999, Kraaijeveld et al. 2001).

Kao (2006), showed that where the transmission rate per contact β is fixed, coexistence can occur between strains that differ in $R_0(\lambda)$, but only at the extrema of exploitation strategies. Here, we show that even where β^λ varies between strains, strains with greater $R_0(\lambda)$ do not always win outright in the evolutionary 'arms race'. This coexistence is possible as the host population represents a structured resource for the parasite: though all parasites can possibly infect every host, certain hosts are more likely to be infected by certain parasites.

Where $\beta^0\langle n^2\rangle < \beta^1$, the heterogeneous transmission route of infection loses its advantage over the homogeneous one and cannot coexist: not only does it have a lower equilibrium prevalence in the single-strain model, but also a lower $R_0(\lambda)$. Those hosts with high ξ are still more readily infected by the heterogeneous transmission hosts, but they are too few to support an epidemic. The appendix considers where susceptibility and infectiousness, though heterogeneous, are uncorrelated. Here, there is no advantage to exploiting host heterogeneity in terms of increased R_0 (as demonstrated in Appendix 1), but the disadvantage due to lower equilibrium prevalence would remain.

In this model, the relationship across strains between mean transmission rate β^λ and λ is linear (Eq. 5). A different functional form here could alter the outcome of the simulations by either strongly favouring or disfavouring intermediate types. The intermediate fitness minimum restricts evolution from low to high λ. Crossing this minimum is slow since the Gaussian distribution of mutation distances used has comparatively short tails, preventing evolution across a fitness minimum where the population size is small (such that few random long-distance events will occur) and σ_λ low. A distribution with wider tails would increase the likelihood of evolution across the fitness minimum, as would environmental variation in the λ trait, which would lessen selection against unfavourable genotypes.

Gandon et al. (2001, 2003) show that disease control strategies (vaccination) can result in evolutionary changes in the parasite vaccinated against. In our model, reduction or removal of transmission through one of the transmission routes will favour selection of parasites transmitting through the other route. This flexibility in the parasite would make it more difficult to eradicate. The model does not allow for evolution in the host species: it would be expected that there is selection pressure against higher values of ξ, in

the absence of any other tradeoffs, which might represent some either physiological or behavioural change in the host population. However, Boots and Knell (2002) suggest that high-risk and low-risk strategies may coexist in the presence of STDs. Future work could involve a coevolutionary model with evolution of this trait.

The branching of an initially similar population into two populations with different genotypes through resource partitioning is likely only for asexually reproducing parasites, as modelled above. Sympatric speciation here is a possible result. With sex or recombination, the continual production of intermediate types would counteract the branching caused by disruptive selection where the population does not mate assortatively (Doebeli and Dieckmann, 2000). The evolution of assortative mating would therefore be a prerequisite for the evolution of divergent transmission strategies.

Maximising infection rate (i.e. R_0) in a susceptible population has been regarded as a 'target' for selection (Anderson and May 1982). However, parasite strains with lower transmission rate can evolve where they can occupy niches left vacant by a resident strain, though they would appear to have lower R_0 when observed spreading through fully susceptible populations. Æsop tells of the quick hare who in the long run, lost the race to the slower tortoise. In parasite populations, the tortoise may not win, but he can at least achieve a dignified tie.

References

Allee, W. C. 1931. Animal aggregations: a study in a general sociology. – Univ. of Chicago Press.

Anderson, R. M. and May, R. M. 1982. Coevolution of hosts and parasites. – Parasitology 85: 411–426.

Anderson, R. M. and May, R. M. 1991. Infectious diseases of humans: dynamics and control. – Oxford Univ. Press.

Arien, K. K., Troyer, R. M., Gali, Y. et al. 2005. Replicative fitness of historical and recent HIV-1 isolates suggests HIV-1 attenuation over time. – Aids 19: 1555–1564.

van Ballegooijen, W. M. and Boerlijst, M. C. 2004. Emergent tradeoffs and selection for outbreak frequency in spatial epidemics. – Proc. Natl Acad. Sci. 101: 18246–18250. doi:10.1073/ pnas.0405682101.

Barthélemy, M., Barrat, A., Pastoras-Satorras, R. et al. 2004. Velocity and hierarchical spread of epidemic outbreaks in scale-free networks. – Phys. Rev. Lett. 92: 178701.

Bonsall, M. B., Hassell, M. P. and Asefa, G. 2002. Ecological tradeoffs, resource partitioning, and coexistence in a host-parasitoid assemblage. – Ecology 83: 925–934.

Boots, M. and Knell, R. J. 2002. The evolution of risky behaviour in the presence of a sexually transmitted disease. – Proc. R. Soc. Lond. B 269: 585–589. doi: 10.1098/ rspb.2001.1932

Bourlière, M., Barberin, J. M., Rotily, M. et al. 2002. Epidemiological changes in hepatitis C virus genotypes in

France: evidence in intravenous drug users. – J. Viral Hepatitis 9: 62–70.

Buckee, C. O'F., Koelle, K., Mustard, M. J. et al. 2004. The effects of host contact network structure on pathogen diversity and strain structure. – Proc. Natl Acad. Sci. 101: 10839–10844.

Dieckmann, U. and Law, R. 1996. The dynamical theory of coevolution: a derivation from stochastic ecological processes. – J. Math. Biol. 34: 579–612.

Diekmann, O., Heesterbeek, J. A. P. and Metz, J. A. J. 1990. On the definition and the computation of the basic reproduction ratio R0 in models for infectious diseases in heterogeneous populations. – J. Math. Biol. 28: 365–382.

Doebeli, M. and Dieckmann, U. 2000. Evolutionary branching and sympatric speciation caused by different types of ecological interactions. – Am. Nat. 156: S77–S101.

Frank, S. A. 1996. Models of parasite virulence. – Q. Rev. Biol. 71: 37–78.

Gandon, S., Mackinnon, M. J., Nee, S. et al. 2001. Imperfect vaccines and the evolution of pathogen virulence. – Nature 414: 751–756.

Gandon, S., Mackinnon, M. J., Nee, S. et al. 2003. Imperfect vaccination: some epidemiological and evolutionary consequences. – Proc. R. Soc. Lond. B 270: 1129–1136.

Gibbens, J. C., Sharpe, C. E., Wilesmith, J. W. et al. 2001. Descriptive epidemiology of the 2001 foot-and-mouth disease epidemic in Great Britain: the first five months. – Vet. Rec. 149: 729–743.

Haydon, D. T., Kao, R. R. and Kitching, R. P. 2004. The UK foot-and-mouth disease outbreak – the aftermath. – Nat. Rev. Microbiol. 2: 675–681.

Kao, R. R. 2006. Evolution of pathogens towards low R0 in heterogeneous populations. J. Theor. Biol. doi:10.1016/j.jtbi.2006.04.003

Kiss, I. Z., Green, D. M. and Kao, R. R. 2006a. The effect of contact heterogeneity and multiple routes of transmission on final epidemic size. – Math. Biosci. 203: 124–136.

Kiss, I. Z., Green, D. M. and Kao, R. R. 2006b. Infectious disease control using contact tracing in random and scale-free networks. – J. R. Soc. Interface 3:55–62. doi:10.1098/rsif.2005.0079.

Kraaijeveld, A. R., Hutcheson, K. A., Limentani, E. C. et al. 2001. Costs of counter-defences to host resistance in a parasitoid of *Drosophila*. – Evolution 55: 1815–1821.

Li, J., Ma, Z., Blythe, S. P. et al. 2003. Coexistence of pathogens in sexually-transmitted disease models. – J. Math. Biol. 47: 547–568. doi: 10.1007/s00285-003-0235-5

Liljeros, F., Edling, C. R. and Nunes Amaral, L. A. 2003. Sexual networks: implications for the transmission of sexually transmitted infections. – Microbes Infection 5: 189–196.

Lloyd-Smith, J. O., Schrieber, S. J., Kopp, P. E. et al. 2005. Superspreading and the effect of individual variation on disease emergence. – Nature 438: 355–359.

May, R. M. and Lloyd, A. L. 2001. Infection dynamics on scale-free networks. – Phys. Rev. E 64: 066112.

Maynard Smith, J. and Price, G. R. 1973. The logic of animal conflict. – Nature 246: 15–18.

Messenger, S. L., Molineux, I. J. and Bull, J. J. 1999. Virulence evolution in a virus obeys a tradeoff. – Proc. R. Soc. London B 266: 397–404.

Mylius, S. D. and Diekmann, O. 1995. On evolutionarily stable life histories, optimization and the need to be specific about density dependence. – Oikos 74: 218–224.

Newman, M. E. J. 2002. The spread of epidemic disease on networks. – Phys. Rev. E 66: 016128.

Rand, D. A., Keeling, M. and Wilson, H. B. 1995. Invasion, stability, and evolution to criticality in spatially extended, artificial host-pathogen ecologies. – Proc. R. Soc. Lond. B 259: 55–63.

Read, J. M. and Keeling, M. J. 2003. Disease evolution on networks: the role of contact structure. – Proc. R. Soc. B 270: 699–708.

Schrag, S. J. and Wiener, P. 1995. Emerging infectious disease: what are the relative roles of ecology and evolution? – Trends Ecol. Evol. 10: 319–324.

Schröter, M., Zöllner, B., Schäfer, P. et al. 2002. Epidemiological dynamics of hepatitis C virus among 747 German individuals: new subtypes on the advance. – J. Clin. Microbiol. 40: 1866–1868.

Schwartz, N., Cohen, R., ben-Avraham, D. et al. 2002. Percolation in directed scale-free networks. – Phys. Rev. E 66: 015104(R).

Thrall, P. H. and Antonovics, J. 1997. Polymorphism in sexual versus non-sexual disease transmission. – Proc. R. Soc. B 264: 581–587.

Wilson, W. G., Osenberg, C. W., Schmitt, R. J. et al. 1999. Complementary foraging behaviors allow coexistence of two consumers. – Ecology 80: 2358–2372.

Yorke, J. A., Hethcote, H. W. and Nold, A. 1978. Dynamics and control of the transmission of gonorrhea. – Sexually Transmitted Diseases 5: 51–56.

Appendix I

In the following derivation of R_0 for the general SIS model, we adopt the convention $\langle a^n \rangle = \int_\Omega \xi^n a_\xi d\xi$. We define I as earlier, and J as follows:

$$I(t) = \int_\Omega i_a da$$

$$J(t) = \int_\Omega a i_a da = \langle i^1 \rangle.$$

The derivatives dI/dt and dJ/dt can be obtained from Eq. 4:

$$\frac{dI}{dt} = \int_\Omega \frac{di_a}{dt} da$$

$$= \int_\Omega \lambda\beta^1 s_a I da + \int_\Omega (1-\lambda)\beta^0 a s_a J da - \int_\Omega \gamma i_a da$$

$$\frac{dJ}{dt} = \int_\Omega a \frac{di_a}{dt} da$$

$$= \int_\Omega a\lambda\beta^1 s_a I da + \int_\Omega a(1-\lambda)\beta^0 a s_a J da - \int_\Omega a\gamma i_a da$$

which simplify to give

$$\frac{dI}{dt} = I(\lambda\beta^1 S - \gamma) + J((1-\lambda)\beta^0 \langle s^1 \rangle)$$

$$\frac{dJ}{dt} = I(\lambda\beta^1 \langle s^1 \rangle) + J((1-\lambda)\beta^0 \langle s^2 \rangle - \gamma).$$

The dominant eigenvalue of the Jacobian matrix of I and J represents the intrinsic rate of natural increase r of the infectious population when I →0. Here, r =0 represents the transition from a stable to an unstable disease-free state. Assuming that $R_0 - 1 = r/\gamma$, then the following equation for R_0 is obtained:

$$R_0(\lambda, s) = \left(\lambda \beta^1 S + (1 - \lambda) \beta^0 \langle s^2 \rangle \right.$$
$$\left. + \sqrt{\left[\lambda \beta^1 S - (1 - \lambda) \beta^0 \langle s^2 \rangle \right]^2 + 4\lambda(1 - \lambda)\beta^1 \beta^0 \langle s^1 \rangle^2} \right) \Big/ 2\gamma$$

This equation reduces to give the following definitions of R_0 used to generate Fig. 2:

$$R_0(0, s*(1)) = \frac{\beta^0}{\gamma} \langle s^2 \rangle \qquad (8)$$

$$R_0(1, s*(0)) = \frac{\beta^1}{\gamma} S. \qquad (9)$$

Consider also the equivalent to Eq. 3 where individuals have separate infectiousness ξ and susceptibility ς, rather than a single property determining both. The numbers of such individuals in class a are then denoted by $a_{\xi\varsigma}$.

$$\frac{di_{\xi\varsigma}}{dt} = \beta\varsigma s_{\varsigma\varsigma} \int\int_\Omega xi_{xy}dxdy - \gamma i_{\xi\varsigma} \quad \xi, \varsigma \in \Omega$$

Following the approach above, with

$$I(t) = \int\int_\Omega \frac{di_{\xi\varsigma}}{dt} d\xi d\varsigma$$

$$J(t) = \int\int_\Omega \xi \frac{di_{\xi\varsigma}}{dt} d\xi d\varsigma,$$

and adopting the convention $\langle f \rangle$ for the expectation of f for the susceptible population, we obtain

$$\frac{dI}{dt} = J\beta \int\int_\Omega \varsigma s_{\xi\varsigma} d\xi d\varsigma - I\gamma = -\gamma I + \beta\langle\varsigma\rangle J$$

$$\frac{dJ}{dt} = J\left(\beta \int\int_\Omega \xi\varsigma s_{\xi\varsigma} d\xi d\varsigma - \gamma \right) = (\beta\langle\xi\varsigma\rangle - \gamma)J$$

From this, the following expression from R_0 can be obtained from the Jacobian matrix:

$$R_0 = \frac{\beta}{\gamma} \langle \xi\varsigma \rangle.$$

Where $\xi = \varsigma$ for all individuals, then Eq. 8 above is recovered. Where ξ and ς are uncorrelated across individuals, then $\langle\xi\varsigma\rangle = \langle\xi\rangle\langle\varsigma\rangle = 1$ and Eq. 9 is recovered (compare Schwartz et al. 2002). Between these two extremes, the increase in R_0 depends upon the strength of the correlation.